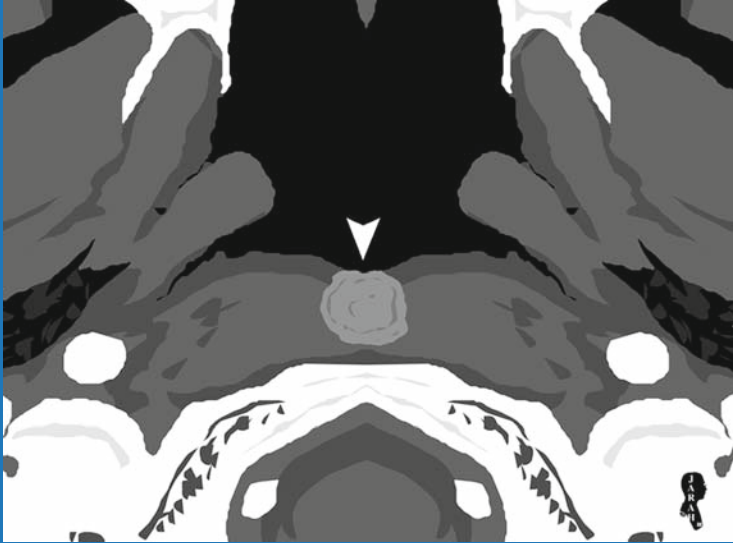


The Head and Neck



CONTENTS

2.1	Eagle Syndrome	36
2.2	Hyperostosis Frontalis Interna	37
2.3	Craniofacial Fibrous Dysplasia and Its Anomalies	38
2.4	Gardner Syndrome	41
2.5	Choanal Atresia	42
2.6	Congenital Cystic Lesions of the Head and Neck	43
2.7	External Auditory Canal Atresia	49
2.8	Congenital Anomalies of the Internal Ear (Congenital Hearing Loss)	50
2.9	Hearing Loss Syndromes	53
2.10	Petrous Bone Vascular Anomalies	56
2.11	Orbital Anomalies	59
2.12	Congenital Cholesteatoma	64

2.1

Eagle Syndrome

Eagle syndrome (ES) is a disease characterized by cervicofacial pain caused by elongation of the styloid process, which occurs due to extensive ossification of the stylohyoid ligament (Fig. 2.1.1). ES is noted to occur in some patients with a previous history of tonsillectomy.

The disease has an incidence of 4% in the general population, with a female predominance. The typical ES patient is female between 30 and 50 years of age with an elongated styloid process and cervicofacial pain.

ES can be asymptomatic, while some patients present with cervicofacial pain in the distribution of the carotid artery, neuralgia of the pharynx, dysphagia, and alteration in taste. Other patients present with chronic headaches with pain in the ophthalmic and the occipital regions when they turn their heads. This pain is classically seen due to bilateral internal carotid artery compression.

The key diagnostic presentations of ES according to otolaryngologists include a patient with throat pain radiating to the ear post tonsillectomy and a patient with a throbbing pain through either the external or the internal carotid artery distribution.

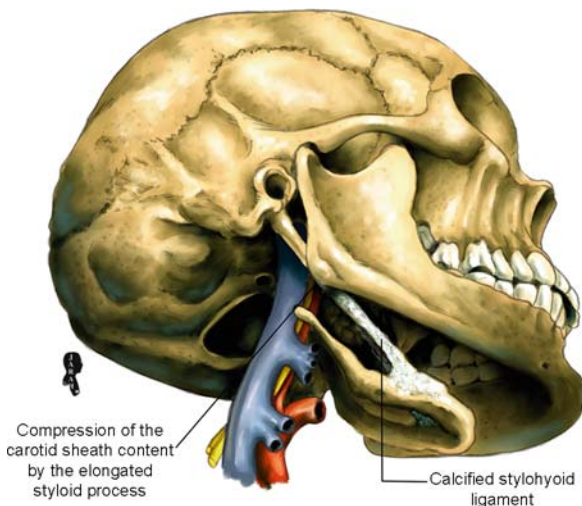


Fig. 2.1.1. Illustration of a calcified stylohyoid ligament with elongation of the temporal styloid process. The calcified ligament presses over the vascular and neural contents of the carotid sheath

Symptoms are believed to be caused by compression of the external carotid artery, internal jugular vein, or cranial nerves (9, 10, and 11) by the deviated, calcified stylohyoid ligament, or by a fibrous tissue scar post tonsillectomy.

Signs on Radiographs

Lateral plain radiographs of the skull and neck show elongation of the temporal styloid process until it reaches the hyoid bone (classic sign) (Fig. 2.1.2).

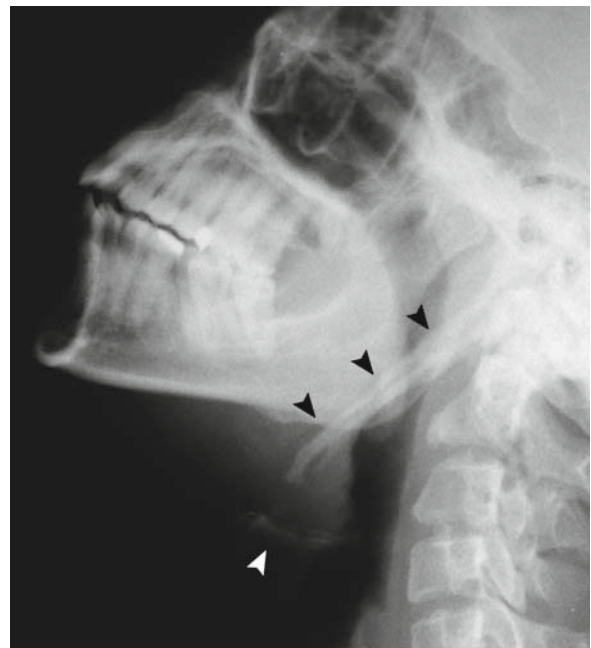


Fig. 2.1.2. Lateral plain radiograph of the neck showing the elongated temporal styloid process with the calcified stylohyoid ligament (black arrowheads) reaching up to the hyoid bone (white arrowhead)

For Further Reading

1. Gustavo M et al. Three-dimensional identification of vascular compression in eagle's syndrome using computer tomography: Case report. *J Oral Maxillofac Surg* 2008;66:169–176
2. Beder E et al. Current diagnosis and transoral surgical treatment if eagle's syndrome. *J Oral Maxillofac Surg* 2005; 63:1742–1745
3. Mendelson AH et al. Heterogeneity in the clinical presentation of eagle's syndrome. *Otolaryngol Head Neck Surg* 2006; 134:389–393

2.2

Hyperostosis Frontalis Interna

Hyperostosis frontalis interna (HFI) is a benign normal variant of unknown cause characterized by increased thickness of the trabecular bone of the inner vault of the skull affecting the frontal bone. HFI is a progressive and symmetrical process. It has an incidence of 4–5% in the general population. HFI affects women more than men (up to 40% of cases are seen in postmenopausal women).

Patients with HFI may suffer from headache and neuropsychiatric diseases like epilepsy and dementia. Additionally, HFI has been linked to various endocrinopathies such as diabetes mellitus, toxic goiter, and acromegaly.

Morgagni syndrome: a syndrome characterized by obesity, hirsutism (abnormally excessive hair growth), and HFI.

Signs on Plain Skull Radiographs

There is increased thickening of the inner frontal bone (Fig. 2.2.1).



Fig. 2.2.1. A lateral plain radiograph of the skull shows increased bone thickness in the inner surface of the frontal bone (arrowheads)

Signs on CT

Bilateral, almost symmetrical increased thickening of the inner surface of the frontal bone (Fig. 2.2.2).

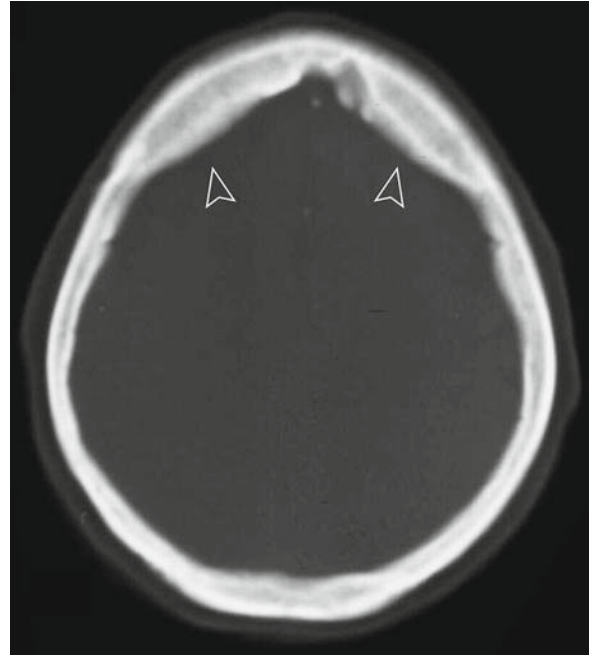


Fig. 2.2.2. Axial bone-window CT of the skull shows bilateral increase in the thickness of the inner surface of the frontal bone (arrowheads)

For Further Reading

1. Kocabas H et al. Hyperostosis frontalis interna in a patient with giant cell arteritis. *Mod Rheumatol* 2008;18:181–183
2. Chaljub G et al. Unusually exuberant hyperostosis frontalis interna: MRI. *Neuroradiology* 1999;41:44–45
3. Harding FE. Endocrinopathies associated with hyperostosis frontalis interna. *Am J Med* 1949;6(3):329–335

2.3

Craniofacial Fibrous Dysplasia and Its Anomalies

Craniofacial fibrous dysplasia (CFD) is a disease of unknown origin characterized by replacement of the normal bone and bone marrow by fibrous tissues; it affects any bone in the body.

The disease may affect a single bone (called monostotic fibrous dysplasia) or multiple bones (called polyostotic fibrous dysplasia). CFD occurs in 20% of the general population and is commonly associated with the polyostotic form of the disease. The peak incidence is in children and teenagers (before 30 years of age).

The common presentation is a young child brought in by the parents due to facial swelling and asymmetry. Other clinical presentations involve unilateral proptosis due to orbital bone involvement. Visual disturbance may occur as a result of optic nerve compression secondary to optic foramen stenosis by the expanded, sclerotic bones.

Leontiasis ossea: is a rare form of CFD with extensive maxillary involvement leading to maxillary encroachment on the orbital cavities, mouth, and paranasal sinuses, which produces a wide facial appearance likened to a lion's face (Fig. 2.3.1, 2.3.4, and 2.3.5).



Fig. 2.3.1. Illustration of a patient with bilateral leontiasis ossea. Note the wide face that looks like the characteristic face of a lion. Also, note the hypertelorism resulting from distension of the facial bones

McCune-Albright syndrome: is a rare disease affecting young female subjects characterized by polyostotic fibrous dysplasia, precocious puberty, and skin hyperpigmentation.

Cherubism: is a term used to describe symmetrical involvement of the maxilla and mandible producing bilateral, progressive swelling of the cheeks (Fig. 2.3.2). It can be caused by CFD and giant cell lesions (Fig. 2.3.3). Cherubism is a benign condition with an autosomal dominant mode of inheritance. Typically, it presents around the age of 7 years and tends to regress after adolescence.

Mazabraud syndrome: is a rare disease characterized by the association of polyostotic fibrous dysplasia with intramuscular myxoma.

Signs on Plain Radiographs

Diffuse thickening and sclerosis of the affected facial bones with classic "ground glass" appearance due to the fibrous matrix nature of the disease.



Fig. 2.3.2. Illustration of a young girl with bilateral full cheeks (cherubism). Cherubism is a term used to describe bible drawings of children with full cheeks

Fig. 2.3.3. Axial and coronal bone-window CT scan of a patient with unilateral fibrous dysplasia of the mandible (arrows). Bilateral involvement of the mandible by fibrous dysplasia is termed cherubism

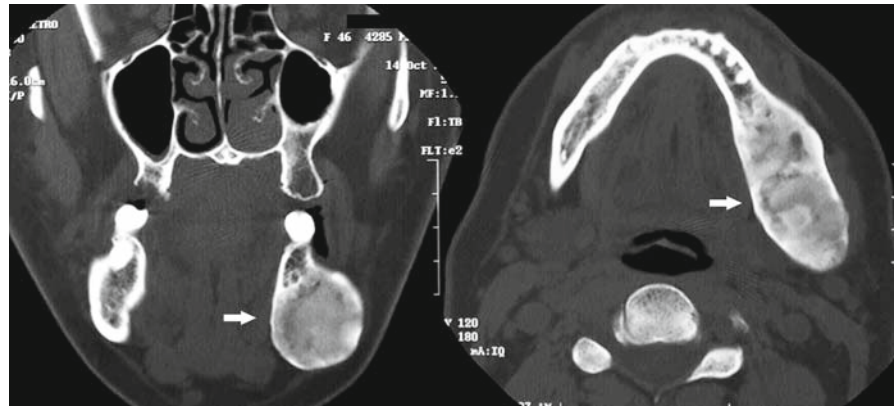


Fig. 2.3.4. Axial bone-window CT images of a patient with leontiasis ossea. **a** Note the extensive involvement of the left foramen rotundum, greater wings of the sphenoid, petrygopalatine fossa and its canal, basisphenoid bone, posterior ethmoid air cells, and clivus by fibrous dysplasia (arrows). The lesion has a classic “ground glass” appearance. **b** Extensive involvement of the left maxillary sinus, zygomatic bone, and the petrygoid plates is clearly seen (arrows). Note the left facial distension (open arrowheads) caused by the lesion compared with the normal right side

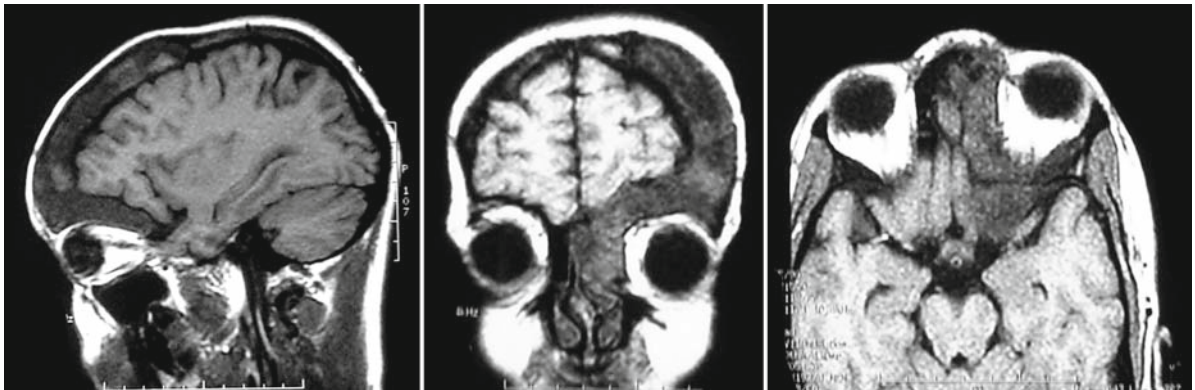
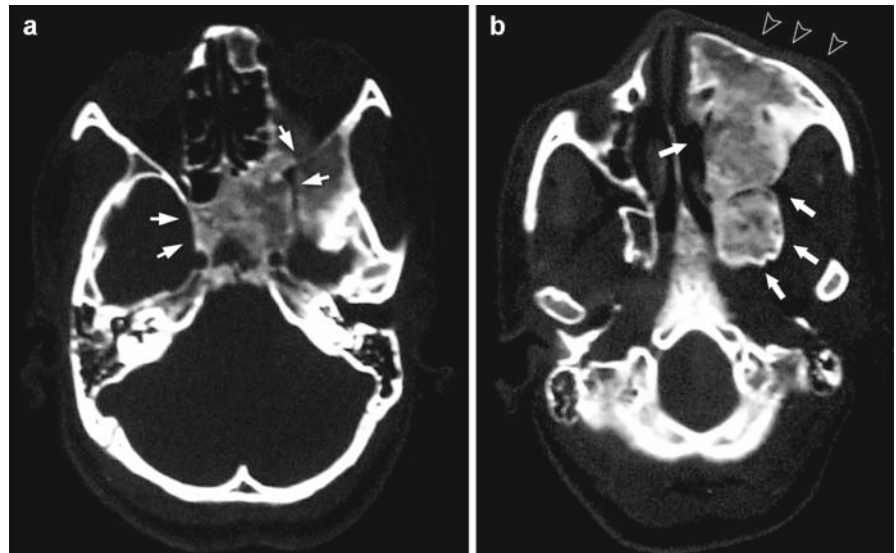


Fig. 2.3.5. Sagittal, coronal, and axial T1-weighted MR images show extensive fibrous dysplasia involving the left clavarium and the left paranasal sinuses in another patient with CFD. Note the hypointense signal of the lesion due to its fibrous content

Signs on CT

- The involved bones appear expanded with intact inner and outer surfaces (Fig. 2.3.4).
- The bone may show osteolytic features or sclerotic features depending on the matrix calcification rate.
- **Small orbit sign:** a decrease in the size of the orbit due to bony orbit expansion.

Signs on MRI

The bones show expansion with low signal intensity in T1-weighted sequence with inhomogeneous gadolinium enhancement due to the fibrous nature of the lesion (Fig. 2.3.5).

Differential diagnosis:

- **Ossifying fibroma of the head and neck** (localized to one bone and rarely crosses to another bone. It also has a female predominance, with age of presentation in the third to fourth decade).

- **Paget disease of the skull** (found in older age-group and affects both the facial bones and the clavarium extensively, in contrast to fibrous dysplasia which can extensively affect the facial bones without affecting the clavarium).

For Further Reading

1. Jain V et al. Radiographic, CT and MRI features of cherubism. *Pediatr Radiol* 2006;36:1099–1104
2. Carbral CEL et al. Polyostotic fibrous dysplasia associated with intramuscular myxoma: Mazabraud's syndrome. *Skeletal Radiol* 1998;27:278–282
3. Yüceer N et al. Polyostotic fibrous dysplasia with craniofacial localization presenting with frontal lobe compression in a 14-year-old Girl. *Acta Neurochir (Wien)* 1999;141:203–207
4. Mendonca JJ et al. Fibrous dysplasia of the mandible: Surgical treatment with platelet-rich plasma and a cortico-cancellous iliac crest graft-report of a case. *Oral Surg Oral Med Oral Pathol Oral Radiol Endod* 2008;105: e12–e18
5. Sherman NH et al. Fibrous dysplasia of the facial bones and mandible. *Skeletal Radiol* 1982;8:141–143
6. Maramatton BV. Leontiasis ossea and post traumatic cervical cord contusion in polyostotic fibrous dysplasia. *Head Face Med* 2006;2:24. doi 10.1186/1746–160x-2–24

2.4

Gardner Syndrome

Gardner syndrome is a rare, hereditary disease characterized by intestinal polyposis (made of adenomas), multiple osteomas (mainly in the jaw), and multiple cutaneous and subcutaneous lesions (epidermoid cysts and desmoid tumor).

The intestinal polyposis is hereditary with a 100% chance of malignant transformation if not treated.

Osteoma is a benign bony island that can be made up of compact (ivory) or trabecular bone. In Gardner syndrome, osteomas are commonly found in the jaw and the skull. In the jaw, the most characteristic and diagnostic locations for Gardner syndrome osteomas are the mandibular angle or its inferior surface (Fig. 2.4.1). Mandibular osteomas can be the initial sign and symptom of Gardner syndrome.

The disease commonly presents with dental abnormalities (30%) such as dental hypoplasia, supernumerary teeth, and compound odontomas.

Epidermoid cysts present in the face, scalp, and extremities in around 50% of cases.



Fig. 2.4.1. Illustration of the classic locations of Gardner syndrome osteomas, at the angle of the mandible and its inferior surface

Desmoid tumor is a benign fibrous soft-tissue proliferation that occurs in the skin or inside the abdomen. It has no malignant tendency; however, it has an aggressive infiltration of the adjacent tissues and tends to reoccur after surgical excision. It is seen in 8.9% of cases.

Congenital hypertrophy of the retinal pigment epithelium (CHRPE) can be seen in up to 85% of cases.

Signs on Plain Radiographs

- Osteomas of the skull, angle of the mandible, or its inferior surface (Fig. 2.4.2).
- Dental anomalies, hypoplasia, and unruptured teeth.
- Cortical thickening (hyperostosis) in the long bones.

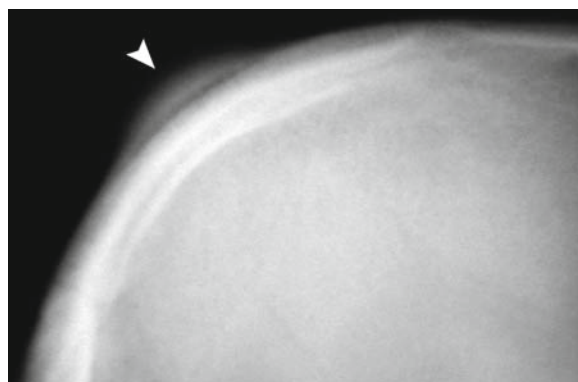


Fig. 2.4.2. Plain radiograph of the skull shows ivory osteoma of the clavarium (arrowhead)

For Further Reading

1. Baykul T et al. Multiple huge osteomas of the mandible causing disfigurement related with Gardner's syndrome: Case report. *Auris Nasus Larynx* 2003;30:447–445
2. Butler J et al. Gardner syndrome-review and report of a case. *Oral Oncology EXTRA* 2005;41: 89–92
3. Parks ET et al. Gardner syndrome. *J Am Acad Dermatol* 2001;45:940–942

2.5

Choanal Atresia

Choanal atresia is an uncommon sinusoidal malformation characterized by unilateral or bilateral closure of the communication between the posterior nasal choana and the nasopharynx. The closing ridge is bony in 90% of cases and membranous in 10% of cases.

Up to 50% of neonates with choanal atresia have craniofacial, cardiovascular, or visceral congenital malformations (e.g., CHARGE association). *CHARGE association* is a congenital syndrome characterized by coloboma, heart disease, atresia of the choanae, retarded mental development, genital hypoplasia, and ear anomalies and deafness.

Neonates with bilateral choanal atresia present with respiratory distress in the immediate newborn period. In contrast, unilateral choanal atresia may be diagnosed later in life.

Signs on Plain Radiographs

- Lateral radiographs demonstrate a discrete separation between the air in the nasopharynx and the air in the posterior nasal cavity.
- Contrast material instilled into the nasal cavity in supine position will collect against the obstruction (Fig. 2.5.1).



Fig. 2.5.1. Plain radiograph of the skull base shows contrast material instilled into the nose with collection of the contrast material against an obstructed posterior choana in a patient with bony choanal atresia

Signs on Paranasal Sinus CT

- Axial CT images demonstrate thickening and medial bowing of the lateral wall of the nasal cavity with atresia of the posterior choana. Fusion between the vomer and the palatine bones obstructing the opening to the nasopharynx is usually seen.
- Membranous atresia is seen as an isodense soft-tissue mass closing the passage between the posterior choana and the nasopharynx (Fig. 2.5.2).

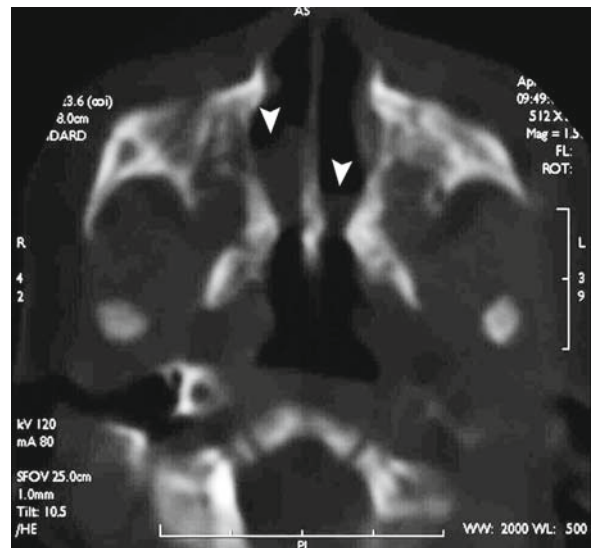


Fig. 2.5.2. Axial bone-window CT of the paranasal sinuses shows bilateral soft-tissue density masses blocking the passage of the posterior choana in a patient with soft-tissue choanal atresia (arrowheads)

For Further Reading

1. El-Sawy H et al. Bilateral choanal atresia and paranasal sinus hypoplasia in an adult patient with hypogammaglobulinaemia. *Eur Arch Otorhinolaryngol* 2006;263:1136–1138
2. Koletzko B and Majewski F. Congenital anomalies in patients with choanal atresia: CHARGE-association. *Eur J Pediatr* 1984;142:271–275

2.6

Congenital Cystic Lesions of the Head and Neck

Cystic lesions of the head and neck are usually either congenital or acquired in origin. Acquired lesions are a result of inflammatory conditions or, rarely, neoplastic (e.g., Warthin tumor). Most of the cystic lesions are seen in children, and are diagnosed according to their location.

The Pharyngeal Bursa of Luschka

The pharyngeal bursa of Luschka is a median formation that projects in the midline of the nasopharynx between the longus capitis muscles. It is seen in 7% of the population as an incidental, asymptomatic finding. When the bursa becomes infected, it is called “Thornwaldt cyst.”

Signs on CT and MRI

The scan shows a median recess that contains air between the longus capitis muscles (Fig. 2.6.1).



Fig. 2.6.1. Axial head CT illustration shows a median recess located between the longus capitis muscles representing the pharyngeal bursa of Luschka (arrowhead)

Thornwaldt Cyst (Pharyngeal Bursitis)

Thornwaldt cyst results from obstruction of the pharyngeal bursa due to inflammation or trauma. The cyst is typically located midline in the posterosuperior wall of the nasopharynx.

Signs on CT

- A hyperdense cyst located at the midline between the longus capitis muscles and the posterior wall of the nasopharynx. The cyst does not enhance after contrast material administration (Fig. 2.6.2).
- Occasional calcifications may occur.



Fig. 2.6.2. Axial noncontrast-enhanced head CT illustration shows a round, hyperdense mass located between the longus capitis muscles representing a Thornwaldt cyst (arrowhead)

Signs on MRI

- The cyst is located in the mid-posterior wall of the nasopharynx with high T1 and high T2 signal intensities (the high signal in T1 depends on the protein content of the cyst).
- The cyst wall may enhance after injection of contrast material.

Differential Diagnosis

- Mucosal cyst (exhibits low T1 signal intensity on MR images and is usually located in the lateral recess).
- Branchial cleft cysts (by their location).

Thyroglossal Duct Cyst

The thyroid gland develops medially at the base of the tongue and then descends anterior to the hyoid bone along the thyroglossal duct to its normal position. When the thyroglossal duct fails to obliterate, it results in the formation of a median or paramedian cyst. The normal thyroglossal duct extends from the foramen cecum at the base of the tongue to the lower neck region where the thyroid bed is. It is obliterated between the fifth and sixth weeks of gestation.

Thyroglossal duct cysts account for up to 70% of all cystic malformations in the neck. Up to 50% are located at the hyoid bone, 25% below the hyoid and 25% above it.

Signs on CT

- Typically, the scan shows a median–paramedian cyst located at the level of the hyoid bone with no contrast enhancement (Fig. 2.6.3).
- The cyst typically splits the two anterior bellies of the digastric muscles.
- Ring contrast enhancement may be seen in cases of infected cyst.

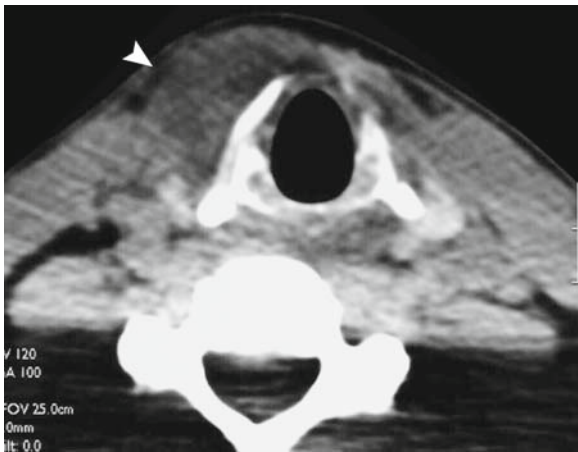


Fig. 2.6.3. Axial postcontrast neck CT shows a right paramedian hypodense cystic lesion at the level of the larynx representing a thyroglossal duct cyst (arrowhead)

Cystic Hygroma (Lymphangiomatosis)

Lymphangiomatosis is a rare disorder of unknown origin characterized by diffuse proliferation of the lymphatic channels in the body with obstruction of

lymphatic drainage. It involves lymphatic proliferation in the bones and viscera. The disease affects children and young adults.

There are three forms of lymphangiomatosis:

- **Cystic form:** this form is known as “cystic hygroma,” and most commonly occurs in the neck or the axilla in children.
- **Capillary form:** this form affects the skin.
- **Cavernous form:** this form affects the bone, soft tissues, and the viscera.

Cystic hygroma is usually diagnosed before 2 years of life. Typically, the cyst grows in size as the child grows.

Cystic hygroma can be associated with genetic syndromes such as Turner syndrome, trisomy 21, 13, and 18.

Signs on CT and MRI

- Cystic hygroma appears as a cyst with a thin wall, and a water-dense mass with multiple lobules that do not enhance after injection of contrast material. The mass may show fluid–fluid levels due to intracystic hemorrhage (Fig. 2.6.4).
- The cyst shows ring contrast enhancement if superimposed by infection.
- Hypertrophy of the adjacent bony structures (e.g., mandible) may occur occasionally.

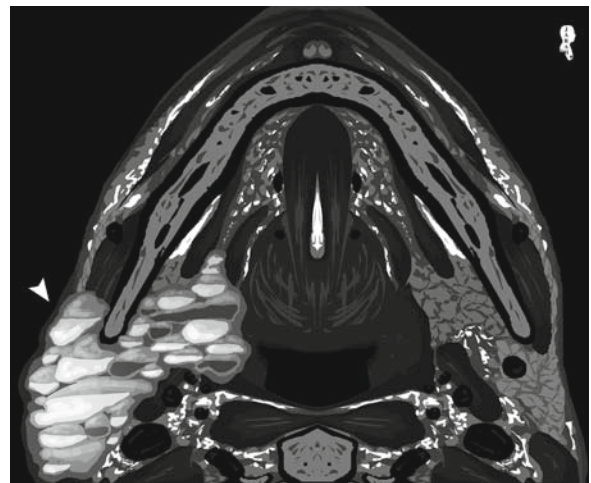


Fig. 2.6.4. Axial T1-weighted MR illustration shows cystic hygroma on the right side with typical fluid–fluid appearance within the cyst, and different intensities due to the cyst content (arrowhead)

Dermoid and Epidermoid Cysts

These lesions are commonly located medially within the neck, and characteristically have thick walls. They are typically midline lesions arising from the floor of the mouth deep to the myelohyoid muscle. Dermoid cysts contain skin, sebaceous glands, and hair follicles. In contrast, epidermoid cysts contain fluid but not fatty material.

Signs on CT and MRI

- These lesions are commonly located medially within the neck, and have thick walls (Fig. 2.6.5).
- On MRI, globules of floating fat within the lesion can produce a characteristic “sack of marbles” appearance or fat–fluid levels (Fig. 2.6.6).
- They can be mistaken for thyroglossal cyst.

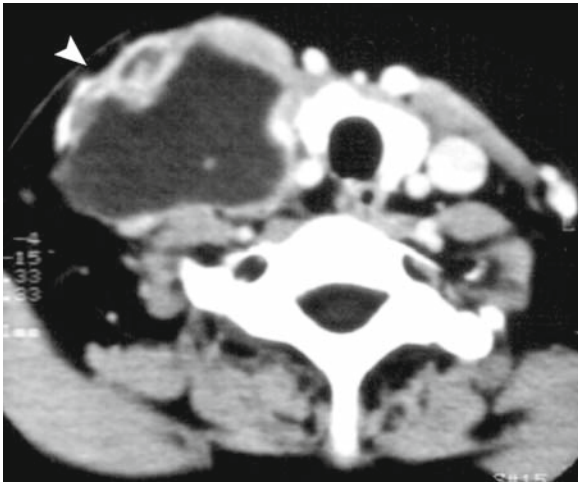


Fig. 2.6.5. Axial postcontrast neck CT shows large paramedian mass with hypodense center and very thick walls. The mass proved to be a malignant epidermoid cyst after biopsy (arrowhead)

Branchial Cleft Cysts

The branchial apparatus comprises structures composed of six pairs of mesodermal arches separated by five pairs of endodermal pharyngeal pouches internally and five pairs of ectodermal branchial clefts externally. They develop between the fourth and fifth weeks of gestation. Branchial cysts are malformations that usually arise from the first four branchial apparatuses.

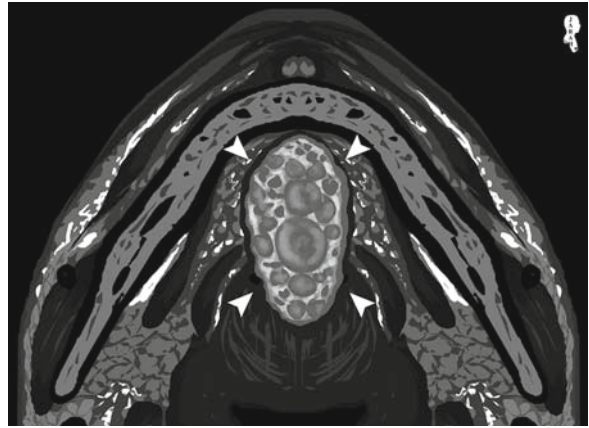


Fig. 2.6.6. Axial T1-weighted MR illustration shows a medial isointense cystic mass containing multiple mildly hyperintense small masses. This appearance is typically seen in dermoid and epidermoid cysts resulting in a “sack of marbles” appearance (arrowheads)

- **First Branchial Cleft Cyst:** This cyst occurs near the external auditory canal or the parotid gland (Fig. 2.6.7). It accounts for 8% of all branchial cleft cysts. Patients present with a mass near the ear with or without recurrent infections.
- **Second Branchial Cleft Cyst:** This cyst occurs anterior to the sternocleidomastoid muscle, lateral to the carotid sheath, and posterior to the submandibular gland and the mandibular edge (Fig. 2.6.8). It accounts for 95% of all branchial cleft cysts. Patients typically present with a nontender lateral neck mass.

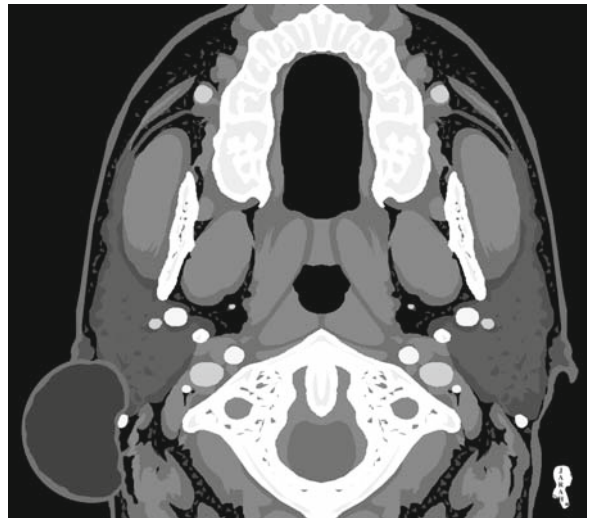


Fig. 2.6.7. Axial postcontrast head CT illustration shows a cyst located near the right external auditory canal and the parotid gland, a typical site for first branchial cleft cyst

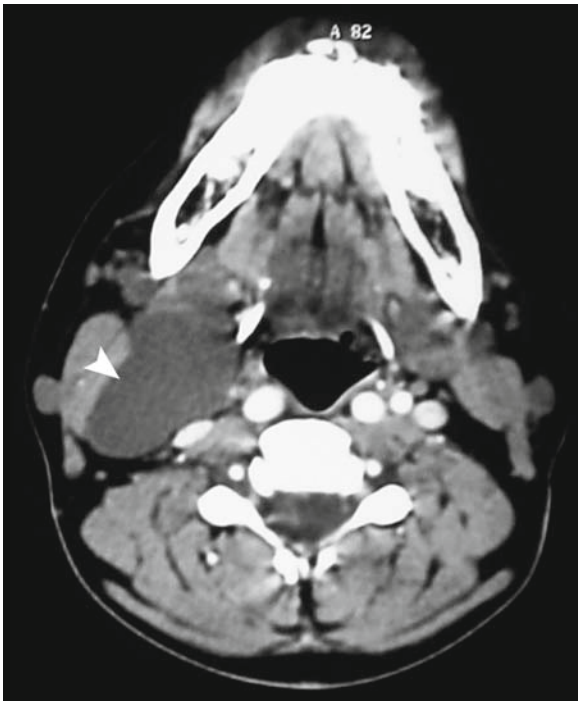


Fig. 2.6.8. Axial postcontrast head CT image shows typical location of the second branchial cleft cyst (*arrowhead*)

- **Third Branchial Cleft Cyst:** This cyst occurs posterior to the internal carotid artery in the upper neck; in the lower neck it can be found in the anterior triangle.

Signs on CT

The cysts appear as hypodense lesions that do not enhance after contrast medium administration. The origin of the cyst is determined according to its location.

Thymic Cysts

Normally, the thymus originates from the third branchial pouch during the fifth week of gestation. It detaches from the pharynx and migrates caudally and medially via the thymopharyngeal duct to reach its normal position in the upper mediastinum. The track of the thymopharyngeal duct extends from the angle of the mandible to the upper mediastinum. Thymic cysts occur due to persistence of remnants of the thymopharyngeal duct (like the thyroglossal duct cyst).

Patients present before 20 years of age complaining of hoarseness, dysphagia, and respiratory distress.

Signs on CT

- The scan shows a hypodense, cystic mass in the upper mediastinum or the lower neck causing tracheal deviation, or exerting mass effect over the adjacent structures.
- The cyst is closely related to the carotid sheath.

Dentigerous (Follicular) Cysts

A dentigerous cyst is one that arises from a tooth after calcification of its crown, and is usually located at the mandibular or the maxillary third molar tooth. The cyst can be large enough to occupy half of the mandible. The peak incidence is between 40 and 60 years of age.

Dentigerous cysts can be associated with mucopolysaccharidosis.

Signs on Radiograph or CT

A cystic lesion of the mandible with an eccentrically placed tooth crown (Fig. 2.6.9).

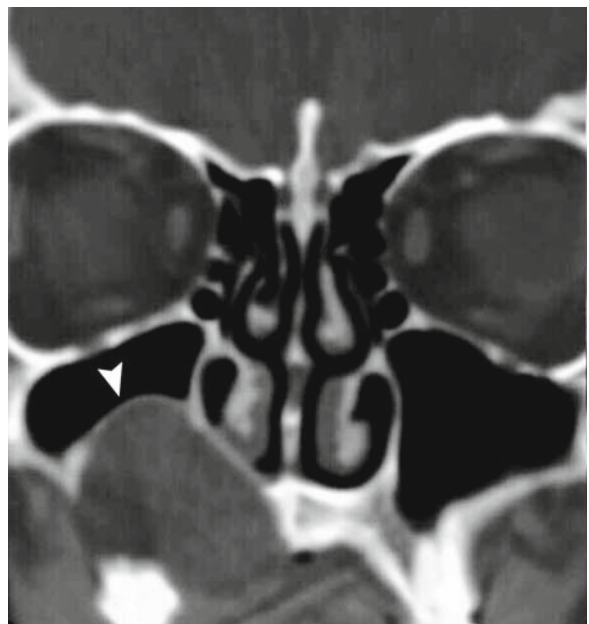


Fig. 2.6.9. Coronal CT of the paranasal sinuses shows a large cyst that arises from the third maxillary molar tooth (dentigerous cyst). The cyst is expanding into more than half the space of the right maxillary sinus (*arrowhead*)

Ranula

The sublingual glands have 8–20 excretory ducts that open below the tongue posterior to the opening of the submandibular duct (of Wharton). Ranula is a retention cyst of the minor salivary gland or the sublingual glands occurring most commonly after trauma or inflammation of the mouth; congenital ranulas are rare.

Typically, the patient is between 25 and 30 years of age with 50% having a history of previous trauma to the mandible.

Ranulas are divided into two types:

- **Simple ranula:** occurs due to obstruction of the salivary gland duct without rupturing. It does not cross the boundaries of the submandibular space.
- **Complicated (diving) ranula:** results from rupture of the gland within the sublingual space with formation of a pseudocyst that can extend into the submandibular space.

Patients often present with painless swelling of the sublingual glands with bluish discoloration (Fig. 2.6.10).

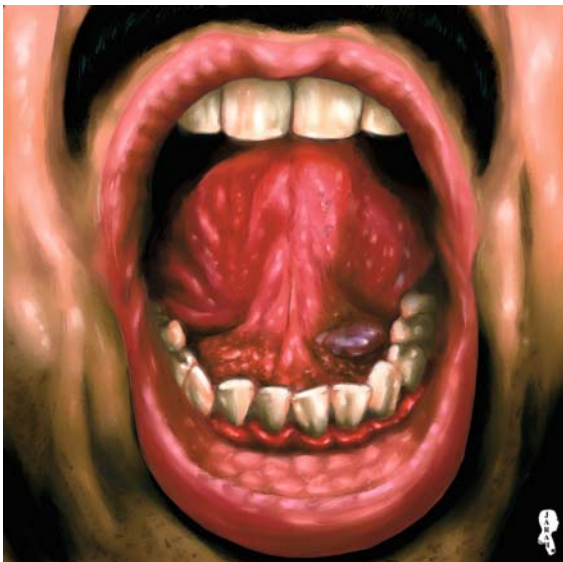


Fig. 2.6.10. Illustration showing the clinical finding in a patient with ranula. Typically, there is a bluish mass found below the tongue, where the sublingual ducts open

Signs on CT

- Simple ranula: the scan shows a hypodense mass located in the sublingual space with a ring enhancement after contrast material injection.
- Complicated ranula appears as a “comet-tail-shaped mass.” The tail is located in the sublingual space and the head is in the submandibular space (Fig. 2.6.11).

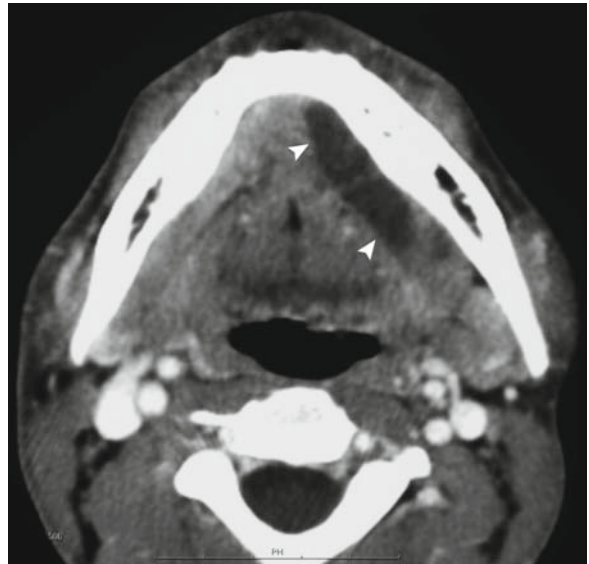


Fig. 2.6.11. Axial postcontrast CT of the floor of the mouth shows complicated (diving) ranula (arrowheads)

Signs on MRI

- The cyst has low T1/high T2 signal intensities with a homogeneous internal architecture. An inhomogeneous internal architecture excludes the diagnosis of ranula.
- The comet-tail sign is seen as a high fluid signal on T2-weighted images within the sublingual space (Figs. 2.6.12 and 2.6.13).
- Extension of the ranula may reach the submandibular space, or further upward into the parapharyngeal space. This free extension occurs because there are no fascial boundaries between the sublingual, submandibular, and parapharyngeal spaces.

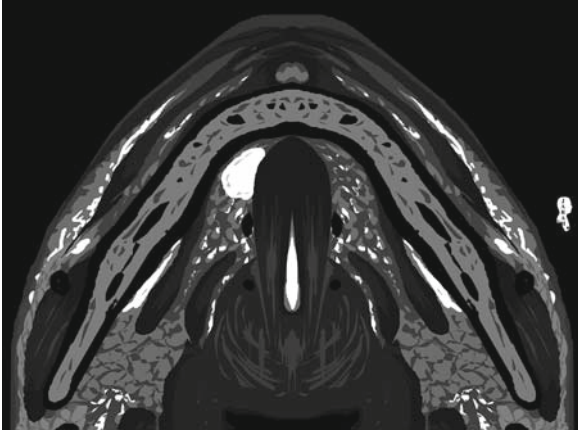


Fig. 2.6.12. Axial T2-weighted MR illustration of the floor of the mouth shows simple ranula seen as a homogeneous mass with defined boundaries

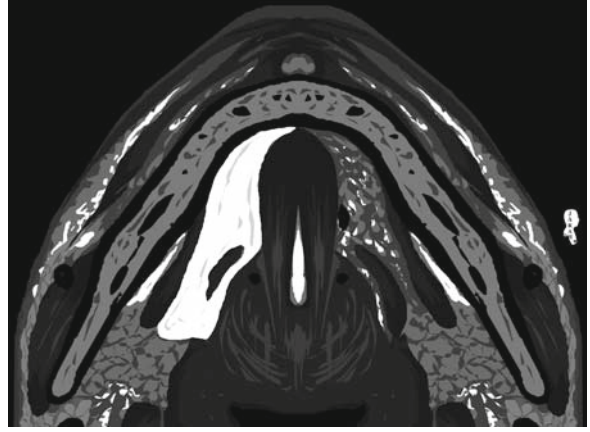


Fig. 2.6.13. Axial T2-weighted MR illustration of the floor of the mouth shows complicated ranula with its “comet tail sign”

For Further Reading

1. Wong KT et al. Imaging of cystic or cyst-like neck masses. *Clin Radiol* 2008;63:613–622
2. Koch BL. Cystic malformations of the neck in children. *Pediatr Radiol* 2005;35:463–477
3. Kurabayashi T et al. MRI of ranulas. *Neuroradiology* 2000; 42:917–922
4. Chong VFH et al. Radiology of the nasopharynx: Pictorial essay. *Australas Radiol* 2000;44: 5–13

2.7

External Auditory Canal Atresia

The external and the middle ear arise from the second and the first branchial arches, and the first branchial cleft in the embryo. External auditory canal (EAC) atresia is characterized by underdevelopment of the external auditory canal.

EAC atresia is often associated with small, deformed pinna (microtia), and deformities in the mandible or the temporomandibular joint (Fig. 2.7.1). EAC atresia is usually bilateral, but unilateral malformation may occur. EAC atresia can be associated with middle ear anomalies (e.g., contracted middle ear cavity) or facial anomalies (e.g., Goldenhar syndrome).

Petrous bone CT is performed to assess bony or soft-tissue blockage and associated middle ear abnormalities (e.g., fused ossicles). A contracted middle ear cavity below 3 mm is incompatible with reconstruction surgery.



Fig. 2.7.1. Illustration shows absence of the entrance of the external auditory canal in a patient with EAC atresia

Signs on Petrous Bone CT

There is absence of the external ear auditory canal, or blockage of the canal by a bone or soft tissue (Figs. 2.7.2 and 2.7.3).

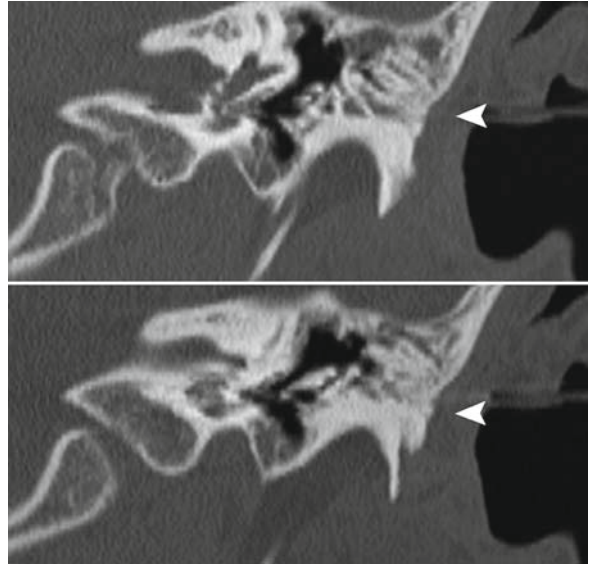


Fig. 2.7.3. Coronal bone-window CT images show absence of the external auditory canal passage on the left ear. The middle ear cavity is blocked by bone with no sign of EAC formation (arrowheads)

For Further Reading

1. Ada M et al. Unusual extension of the first branchial cleft anomaly. *Eur Arch Otorhinolaryngol* 2006;263:263–266
2. Sheykholeslami K et al. Bone-conducted vestibular evoked myogenic potentials in patient with congenital atresia of the external auditory canal. *Int J Pediatr Otorhinolaryngol* 2001;57:25–29

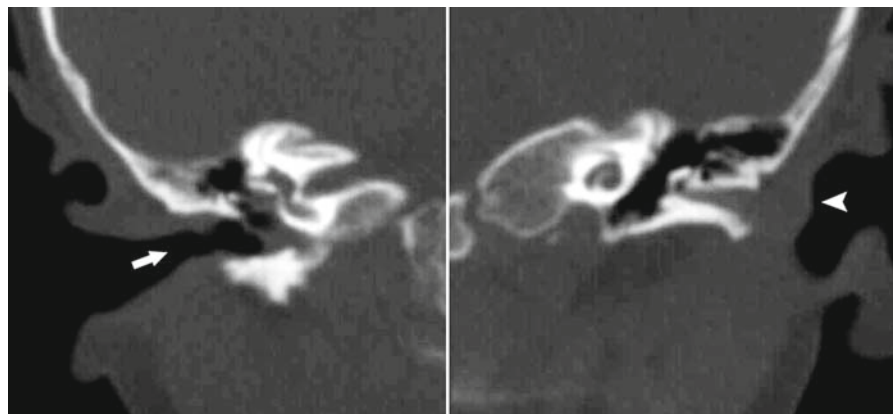


Fig. 2.7.2. Coronal bone-window CT images show soft-tissue blockage of the EAC on the left ear (arrowhead). Note the normal EAC passage on the right ear (arrow)

2.8

Congenital Anomalies of the Internal Ear (Congenital Hearing Loss)

In normal embryological development of the ear, the bony labyrinth evolves between the 4th and 8th week of gestation, grows between from the 8th to the 16th week, and ossifies from the 16th to 24th week. Development of the sensory epithelium occurs after the 25th week. Congenital malformation arises when an insult (e.g., intrauterine infection) occurs between the fourth and eighth weeks of gestation.

Up to 50% of cases of congenital anomalies of the inner ear are due to genetic defects, and the remainder of cases are attributed to intrauterine infections (TORCH), fetal drug ototoxicity, and trauma. Cytomegalovirus is a common infection that causes inner ear anomalies and congenital deafness. Ingestion of ototoxic drugs by pregnant women can lead to congenital hearing loss; examples are alcohol (fetal alcohol syndrome), aminoglycosides, aspirin, erythromycin, and furosamide.

Up to 70% of genetic congenital hearing losses occur as isolated cases, the rest of the genetic cases occur as parts of syndromes.

Presbycusis: is bilateral sensorineural hearing loss due to age. The CT scan shows a normal temporal structure. Malformations that only involve the membranous labyrinth are classified as Alexander and Scheibe deformities. The CT examination of these deformities is normal.

Michel Dysplasia

Michel dysplasia is a term used to describe complete absence of the entire middle ear, including the cochlea, vestibule, and all semicircular canals. The medial wall of the inner ear and the promontory are flat due to inner ear aplasia.

It is a very rare anomaly, and its main differential diagnosis is postmeningitic labyrinthine ossification.

Signs on Petrous Bone CT

The scan shows complete absence of the inner ear (Fig. 2.8.1).

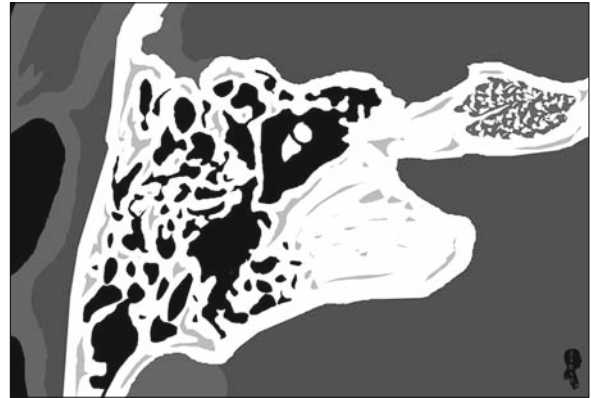


Fig. 2.8.1. Axial petrous bone CT illustration shows complete absence of the cochlea, vestibule, and semicircular canals (Michel anomaly)

Mondini Anomaly

Mondini anomaly is a term used to describe fusion of the apical and the middle cochlear turns making up one cavity, while the basal turn is present.

Up to 20% of patients with Mondini anomaly have other malformations of the vestibule, endolymphatic duct, or semicircular canals.

Patients with Mondini anomaly present with low-frequency hearing deficit, due to fusion of the apical and the middle cochlear turns. In contrast, high-frequency hearing persists due to presence of the basal turn.

Signs on Petrous Bone CT

The scan shows fused apical and middle cochlear turns with loss of the cochlear modiolus (Fig. 2.8.2).

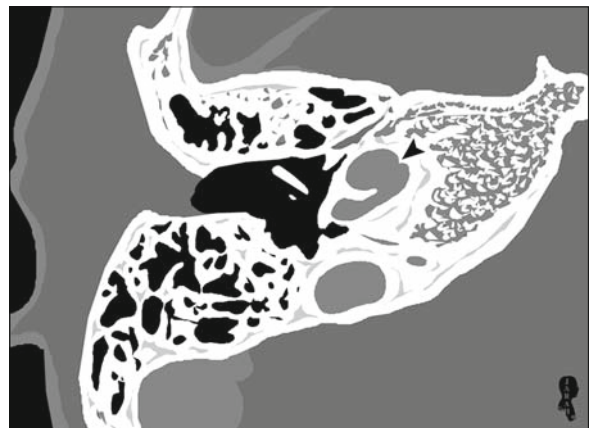


Fig. 2.8.2. Axial petrous bone CT illustration shows Mondini anomaly. Note the fusion between the apical and the middle cochlear turns with absence of the cochlear modiolus (arrowhead)

Common Cavity Deformity

Common cavity deformity is characterized by replacement of the cochlea and the vestibule by a single hollow cavity without internal architecture. It occurs due to inner ear developmental arrest between the fourth and fifth week of gestation.

Signs on Petrous Bone CT

The scan shows one cavity occupying the area of the vestibule and the cochlea (Fig. 2.8.3).

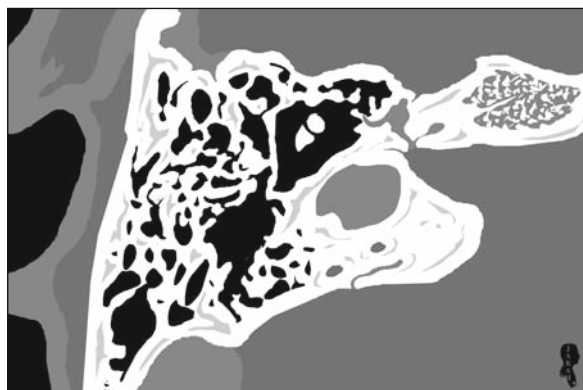


Fig. 2.8.3. Axial petrous bone CT illustration shows the common cavity anomaly. Note the complete fusion between the vestibule and the cochlea to form a single hollow cavity

Semicircular Canal Aplasia/Hypoplasia

Aplasia or hypoplasia of the semicircular canal is an anomaly that arises due to developmental interruption of the semicircular canals during embryogenesis between the sixth and eighth week of gestation. There will be underdevelopment or complete absence of one or more of the semicircular canals; the lateral semicircular canal is the most commonly affected.

Semicircular aplasia can be associated with syndromes such as Goldenhar syndrome and CHARGE association.

Signs on Petrous Bone CT

The scan shows agenesis or underdevelopment of one or more of the semicircular canals.

Semicircular Canal Dehiscence

Semicircular canal dehiscence is a condition characterized by loss of the bony overlay of the posterior or superior semicircular canals. The area of the bony defect is covered only by dura separating the semicircular canal from the cerebrospinal fluid in the cranial fossa. Changes in the pressure within the intracranial space can be transmitted through this defect into the labyrinth resulting in vertigo.

Signs on Petrous Bone CT

The scan shows a bony defect over the superior or the posterior semicircular canal (Fig. 2.8.4).

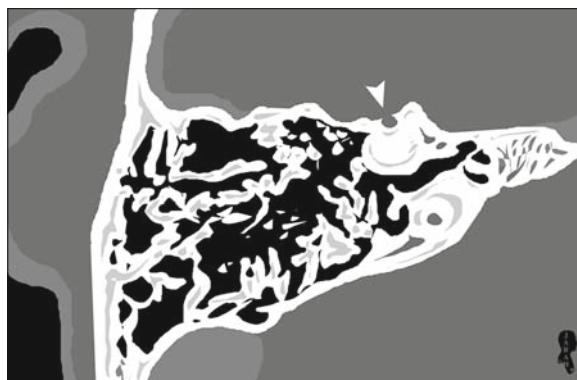


Fig. 2.8.4. Axial petrous bone CT illustration shows loss of the bony covering over the superior semicircular canal, representing semicircular canal dehiscence (arrowhead)

Large Vestibular Aqueduct Syndrome

The vestibular (endolymphatic) aqueduct is a J-shaped bony canal that extends from the medial wall of the vestibule to the posterior surface of the petrous temporal bone. The normal vestibular aqueduct diameter measures

up to 1.5 mm. Congenital enlargement of the vestibular aqueduct beyond this diameter results in progressive, bilateral, sensorineural hearing loss and vertigo, commonly in the younger population.

The vertigo and the sensorineural hearing loss are attributed to damage of the hair cells within the labyrinth due to cerebrospinal fluid pressure fluctuation, which is delivered by the enlarged vestibular aqueduct.

Signs on Petrous Bone CT

The scan shows enlargement of the vestibular aqueduct beyond 1.5 mm in diameter (Fig. 2.8.5).

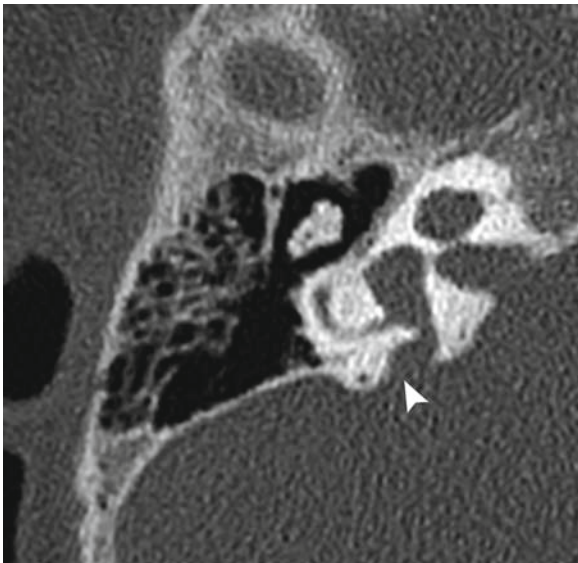


Fig. 2.8.5. Axial petrous bone CT image shows an enlarged vestibular aqueduct (*arrowhead*)

Signs on MRI

The scan shows enlargement of the vestibular aqueduct on T2-weighted images with fluid signal intensity (Fig. 2.8.6).



Fig. 2.8.6. Axial T2-weighted MR image in another patient shows markedly enlarged vestibular aqueduct (*arrowhead*)

For Further Reading

1. Kavanagh KT and Magill HL. Michel dysplasia, Common cavity inner ear deformity. *Pediatr Radiol* 1989;19:343–345
2. Davidson HC. Imaging of the temporal bone. *Neuroimag Clin N Am* 2004;14:721–760
3. Naganawa S et al. Serial MR imaging studies in enlarged endolymphatic duct and sac syndrome. *Eur Radiol* 2002;112:S114–S117
4. Krombach GA. Imaging of congenital anomalies and acquired lesions of the inner ear. *Eur Radiol* 2008;18(2):319–330

2.9

Hearing Loss Syndromes

Hearing loss can occur due to aging, trauma, as well as drug-related and congenital causes. Congenital hearing loss is divided into “syndromic” and “nonsyndromic” types. In the syndromic type, hearing loss occurs as part of a syndrome with other manifestations within the body. There are many syndromes that cause hearing loss as one of their manifestations. Only four of the most common hearing loss syndromes are discussed here.

Waardenburg Syndrome

Waardenburg syndrome is a rare congenital disorder distinguished by characteristic facial features, pigmented abnormalities, and profound, congenital, sensorineural hearing loss (up to 75% of cases).

The disease has an autosomal dominant mode of inheritance, with an incidence of 1:40,000 live births. It accounts for 2% of all congenital hearing loss cases.

Waardenburg syndrome is characterized by (Fig. 2.9.1):

- **Dystopia canthorum** (lateral displacement of the inner canthi, or inner angles of the eyes, plus lateral displacement of the lacrimal puncta).
- **Prominent broad nasal root.**
- **Synophrys** (the eyebrows grow together).

Fig. 2.9.1.

Illustration shows the typical facial features of Waardenburg syndrome. Note the lateral displacement of the medial angles of the eye (*dystopia canthorum*), the prominent broad nasal root, the adjacent eyebrows (*synophrys*), the white forelock, and the two different colors of the iris (*heterochromia irides*)



- **White forelock** (whitish or grayish hair in the front of the head).
- **Heterochromia irides** (two eyes with different colors, or one eye with two different colors in the iris).
- **Congenital bilateral sensorineural hearing loss.**

The disease has four subtypes

- **Waardenburg syndrome type 1:** it is the classic form, and the patient presents with the above-mentioned features.
- **Waardenburg syndrome type 2:** this disease has the same features as type 1 but lacks the dystopia canthorum.
- **Waardenburg syndrome type 3 (Waardenburg-Klein syndrome):** it is a combination of type 1 with upper limb anomalies (e.g., syndactyly).
- **Waardenburg syndrome type 4 (Waardenburg-Shah syndrome):** it is a combination of type 2 with Hirschsprung disease.

ABCD syndrome: is a rare variant expression of Waardenburg-Shah syndrome characterized by albinism, black lock, cell migration disorder of the gut neurocytes, and deafness. The disease has an autosomal recessive mode of inheritance.

Signs on Petrous Bone CT

Abnormalities of the petrous bone are present in 17% of cases, and include aplasia of the semicircular canals and the vestibule.

Pendred Syndrome

Pendred syndrome is an autosomal recessive disease characterized by severe congenital sensorineural hearing loss with iodine organification defect that causes developmental thyroid goiter in infants. The disease accounts for almost 10% of all cases of congenital hearing loss syndromes.

In Pendred syndrome, up to 80% of the thyroid-accumulated iodide is discharged on administration of a substance called “perchlorate”. The perchlorate test is the gold standard test for diagnosing this disease.

The sensorineural hearing loss is often caused by Mondini anomaly or bilateral enlarged vestibular aqueduct syndrome.

Goldenhar Syndrome (Oculo-Auriculo-Vertebral Syndrome)

Goldenhar syndrome is a congenital disorder related to a group of congenital diseases known as “the hemifacial microsomia spectrum.” These diseases are characterized by unilateral or bilateral and often asymmetrical abnormalities of the first and second branchial arch derivatives with facial asymmetry.

Most cases are sporadic and affect one side of the face only.

Goldenhar syndrome is characterized by the following facial features (Fig. 2.9.2):

- Unilateral or bilateral external ear atresia (microtia).
- Unilateral or bilateral mandibular hypoplasia.
- Unilateral or bilateral maxillary flattening.
- **Epibulbar dermoid:** is a benign, white–yellow, or pinkish tumor located on the cornea and the sclera in the temporal quadrants of the eye (characteristic and specific feature of this disease).

Fig. 2.9.2. Illustration shows the typical facial features of Goldenhar syndrome. Note the right unilateral hypoplasia of the mandible, the small right maxilla compared to the left one (unilateral hypoplasia), the small deformed ear on the right side, and the soft-tissue lesion seen in the right eye (*epibulbar dermoid*)



Signs on Petrous Bone CT

- The scan reveals unilateral or bilateral external auditory canal atresia.
- Contracted tympanic cavity and oval window atresia may be seen.

Cogan Syndrome

Cogan syndrome is a rare disease of unknown origin characterized by nonsyphilitic interstitial keratitis with cochleovestibular defects causing sensorineural hearing loss. Interstitial keratitis is an infectious, chronic, nonulcerative inflammation of the cornea with neovascularization.

The disorder is considered to be an autoimmune disease. The autoimmune origin theory is supported by the development of generalized vasculitis affecting the heart coronaries, aorta, and brain vessels in chronic stages of the disease that respond to steroid therapy.

The disease affects adults between 20 and 40 years of age, although it can also affect children in rare cases.

Patients with Cogan syndrome present with bilateral, rapidly progressing hearing loss with tinnitus often combined with vertigo, dizziness, or ataxia. The diagnosis is made based on the clinical combination of eye abnormalities and cochleovestibular disease.

Cogan syndrome is classified according to its ocular manifestations into two types:

- Typical Cogan syndrome: the disease causes nonsyphilitic interstitial keratitis (affects the cornea only).
- Atypical Cogan syndrome: the disease affects the whole globe, presenting with episcleritis, uveitis, and conjunctivitis.

Systemic manifestations of the disease occur in up to 70% of the patients and include fever, malaise, arthralgias, and weight loss.

Cogan syndrome causes acute autoimmune labyrinthitis, which later leads to diffuse fibrosis, cochlear atrophy, and calcifications causing permanent hearing loss. The patient may need cochlear implantation.

Signs on Petrous Bone CT

The cochlea may show signs of thickening, internal soft-tissue density (fibrosis), and in advanced stages cochlear sclerosis (Fig. 2.9.3).

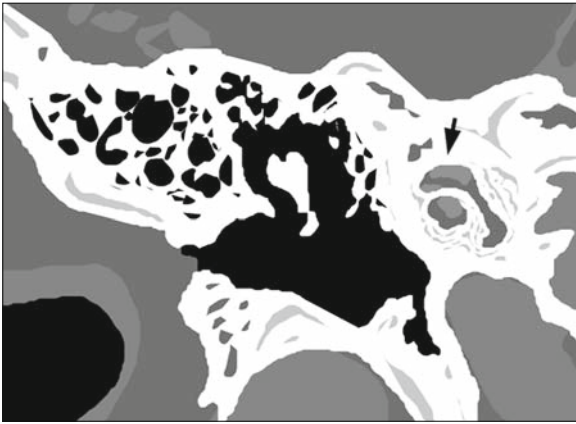


Fig. 2.9.3. Coronal petrous bone CT illustration shows thickening and sclerosis of the cochlea (*arrowhead*), an advanced stage of Cogan syndrome

Signs on MRI

- In active stage of the disease, the membranous labyrinth shows enhancement and high signal intensity on postcontrast T1-weighted images due to inflammation (labyrinthitis) (Fig. 2.9.4a).
- In advanced stages, a hypointense signal is seen in the membranous labyrinth on both T2- and T1-weighted postcontrast images due to calcification and fibrosis (Fig. 2.9.4b).

For Further Reading

1. Lee D et al. Waardenburg syndrome, clinical photographs. *Otolaryngol Head Neck Surg* 1996;114:166–167
2. Rarey KE et al. Intralabyrinthine osteogenesis in Cogan's syndrome. *Am J Otolaryngol* 1986;4:387–390
3. Oysu C et al. Temporal bone imaging findings in Waardenburg's syndrome. *Int J Pediatr Otorhinolaryngol* 2001;58:215–221
4. Robson CD. Congenital hearing impairment. *Pediatr Radiol* 2006;36: 309–324
5. Espeso A et al. The diagnosis of hearing loss in children: Common presentations and investigations. *Curr Paediatr* 2006;16:484–488
6. Phelps PD et al. Radiological malformations of the ear in Pendred syndrome. *Clin Radiol* 1998;53:268–273
7. Ozluk A et al. Carcinomas of the thyroid and breast associated with Pendred's syndrome: Report of a case. *Surg Today, Jpn J Surg* 1998;28:673–674
8. Thomas P. Goldenhar syndrome and hemifacial microsomia: Observations on three patients. *Eur J Pediatr* 1980;133: 287–292
9. Reddy MVV et al. Facio-auricular vertebral syndrome – A case report. *Indian J Hum Genet* 2005;11(3):156–158
10. Olfat M et al. Cogan's syndrome in childhood. *Rheumatol Int* 2001;20:246–249
11. Baumann A et al. Cogan's syndrome: Clinical evolution of deafness and vertigo in three patients. *Eur Arch Otorhinolaryngol* 2005;262:45–49
12. Im GJ et al. Side selection for cochlear implantation in a case of Cogan's syndrome. *J Laryngol Otolaryngol*, 2008;122(3): 310–313
13. Kothari PR et al. ABCD syndrome revisited. *Indian J Hum Genet* 2006;12(3):144–145



Fig. 2.9.4. Axial T1- and T2-weighted MR illustrations show different stages of the vestibular changes in Cogan syndrome. **a** Illustration representing a postcontrast T1-weighted image showing enhanced vestibule due to labyrinthitis (*arrowhead*).



b Illustration representing a noncontrast-enhanced T2-weighted image showing loss of the normal fluid signal within the vestibule due to fibrosis and sclerosis (*open arrowhead*)

2.10

Petrous Bone Vascular Anomalies

Congenital vascular anomalies affecting the petrous bone can be asymptomatic or can result in pulsatile tinnitus. Tinnitus is an auditory sensation perceived in the absence of external stimuli. It is described as buzzing, ringing, or humming. Pulsatile tinnitus is defined as tinnitus that follows the patient's pulse. The most common petrous bone vascular anomalies causing pulsatile tinnitus are the aberrant internal carotid artery, high jugular bulb, and persistent stapedial artery.

Aberrant Internal Carotid Artery

The normal carotid artery courses inside the petrous bone in its carotid canal before entering the middle cranial fossa. Aberrant internal carotid artery (ICA) is a rare condition characterized by presence of the ICA inside the middle (tympanic) ear cavity (Fig. 2.10.1). The condition is explained by two theories:

- **The Alternate Blood Flow Theory:** Normally, the ICA inside its canal is separated from the middle ear cavity via the carotid plate, a bony covering that is less than 0.5 mm in thickness. This plate is perforated by a small branch of the ICA called the “caroti-

cotympanic artery,” which is a remnant of the embryologic “hyoid artery.” The caroticotympanic artery anastomoses over the cochlear promontory with another artery called the “inferior tympanic artery,” a branch of the ascending pharyngeal artery. Both arteries supply portions of the medial wall of the tympanic cavity. Aberrant ICA represents an enlarged inferior tympanic artery anastomosing with an enlarged caroticotympanic artery (persistent hyoid artery) with underdevelopment of the cervical portion of the ICA.

- **The Bony Dehiscence Theory:** This is a rare situation characterized by dehiscence of the carotid plate causing the ICA to herniate inside the middle ear cavity. It is seen on MRI or angiography as a “laterally displaced” ICA.

Clinically, the lesion can be asymptomatic or accompanied by pulsatile tinnitus and conductive hearing loss. It can be mistaken with glomus tympanicum or high jugular bulb on otoscopic examination.

Signs on Petrous Bone CT

The ICA is seen inside the middle ear cavity with no bony plate separating it from the middle ear cavity (Fig. 2.10.2).

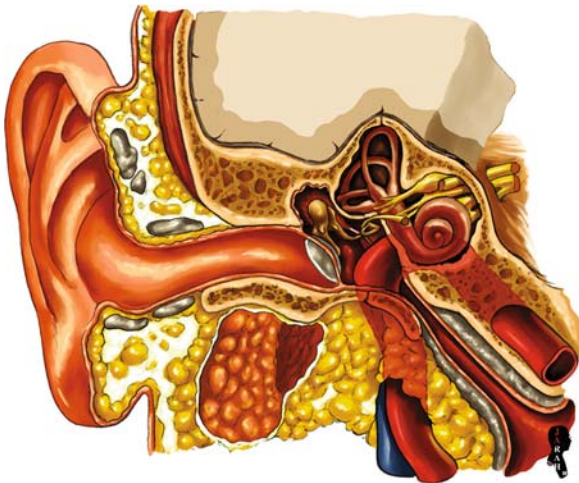


Fig. 2.10.1. Illustration shows aberrant course of the internal carotid artery inside the middle ear cavity

High Jugular Bulb

The jugular bulb is the continuation link between the sigmoid sinus and the internal jugular vein. It lies in the jugular fossa, an oval hollowed area at the internal and inferior surface of the petrous pyramid. The dome of the jugular bulb lies at the floor of the middle ear cavity, at the level of the hypotympanum.

High jugular bulb is a condition characterized by protrusion of the jugular bulb inside the middle ear cavity, commonly due to hypotympanum bone dehiscence (Fig. 2.10.3). The jugular bulb is said to be high if it projects above the bony annulus or the basal turn of the cochlea.

The incidence of high jugular bulb is 5% of the general population; bilateral incidence is found in up to 16% of cases.

Fig. 2.10.2. Axial bone-window petrous bone CT shows aberrant internal carotid artery inside the middle ear cavity on the left side (*arrowhead*). Note the intact carotid bony plate on the right side (*arrow*) and compare it with the left side

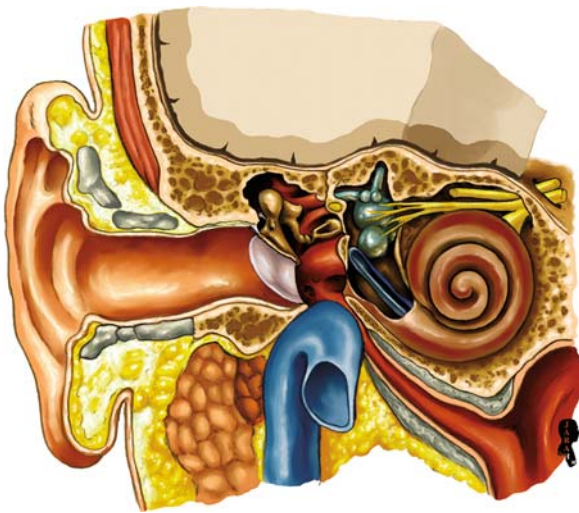
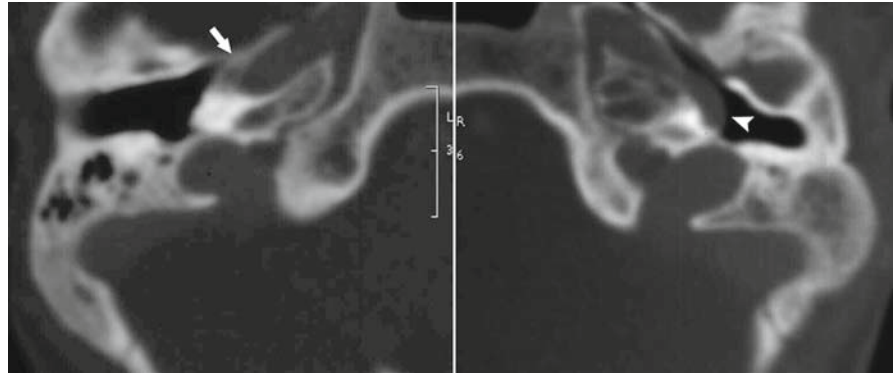


Fig. 2.10.3. Illustration shows bone deficiency (dehiscence) of the hypotympanum with projection of the jugular bulb inside the middle ear cavity at the level of the basal turn of the cochlea (high jugular bulb)

Clinically, it can be asymptomatic in most cases, or accompanied by pulsatile tinnitus. Conductive hearing loss can occur if the bulb encroaches over the tympanic membrane or the ossicles. On otoscopic examination, it is difficult to differentiate high jugular bulb from glomus tympanicum or aberrant ICA.

Signs on Petrous Bone CT

The scan shows a mass with a fluid density projecting inside the middle ear cavity with hypotympanum bone dehiscence (Fig. 2.10.4).

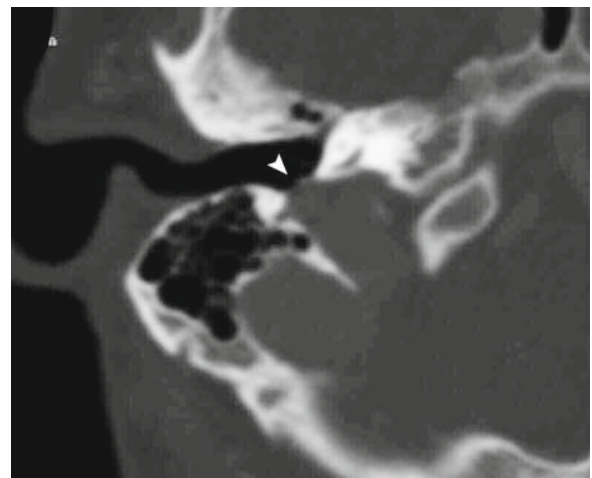


Fig. 2.10.4. Axial bone-window petrous bone CT shows bone dehiscence over the jugular bulb (*arrowhead*)

Persistent Stapedial Artery

Persistent stapedial artery is a rare vascular anomaly that can present in adulthood with pulsatile tinnitus. The stapedial artery is part of the embryonic fetal circulation of the head and neck region. If the fetal artery persists after birth, the middle meningeal artery will not develop, and its arterial territory will be supplied by the stapedial and the ophthalmic arteries.

Persistence of the stapedial artery after birth can be an isolated anomaly or accompanied by an aberrant ICA. It can be seen in cases of trisomy 13, 15, and 21 as well as Paget's disease of the bone.

Signs on Petrous Bone CT

- A mass in the mesotympanum lying near the stapes, which enhances in an arterial fashion after contrast material injection. The key for diagnosis is the relationship of the artery to the stapes (Fig. 2.10.5).
- Foramen spinosum will be absent due to the absence of the middle meningeal artery (Fig. 2.10.6).

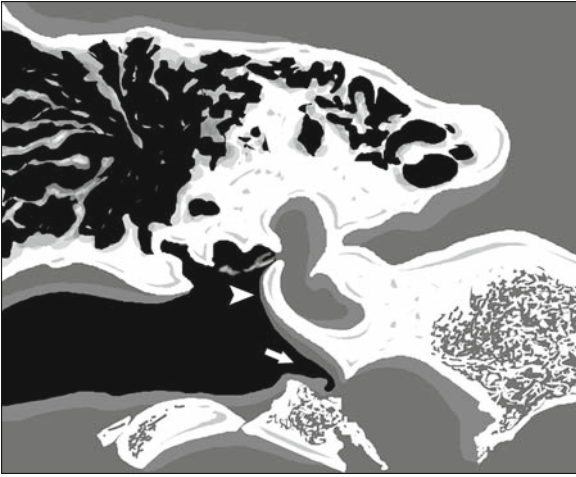


Fig. 2.10.5. Coronal noncontrast-enhanced petrous bone CT illustration shows the persistent stapedial artery with its close relationship to the stapes (*arrowhead*). Note the origin of the artery from the carotid canal (*arrow*)

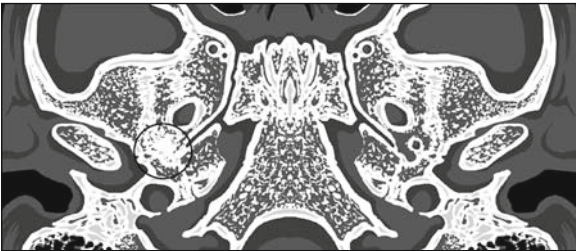


Fig. 2.10.6. Axial base of the skull CT illustration shows absence of the foramen spinosum on the right side (*circle*), a typical finding with persistent stapedial artery

For Further Reading

1. Schwartz JD et al. Aberrant internal carotid artery lying within the middle ear, High resolution CT diagnosis and differential diagnosis. *Neuroradiology* 1985;27:322–326
2. Sauvaget E et al. Aberrant internal carotid artery in the temporal bone, imaging findings and management. *Arch Otolaryngol Head neck Surg* 2006;132(1):86–91
3. Lo WWM. Aberrant carotid artery: Radiologic diagnosis with emphasis on high-resolution computed tomography. *Radiographics* 1985;5(6):985–993
4. Davidson HC. Imaging of the temporal bone. *Neuroimag Clin N Am* 2004;14:721–760
5. Roche PH et al. High jugular bulb in the translabryrinthine approach to the cerebellopontine angle: Anatomical considerations and surgical management. *Acta Neurochir (Wien)* 2006;148:415–420
6. Ozturkcan S et al. Surgical treatment of the high jugular bulb by compressing sinus sigmoideus: Two cases. *Eur Arch Otorhinolaryngol* 2008;265(8):987–991. doi 10.1007/s00405-007-0545-0
7. Lo WWM et al. High-Resolution CT of the jugular foramen: Anatomy and vascular variants and anomalies. *Radiology* 1984;150:743–747
8. Thiers FA et al. Persistent stapedial artery: CT findings. *Am J Neuroradiol* 2000;21:1551–1554
9. Branstetter BF IV. The radiologic evaluation of tinnitus. *Eur Radiol* 2006;16:2792–2802

2.11

Orbital Anomalies

Orbital anomalies are usually seen in infants and children, and are generally rare. Children usually present early in life with visual field disturbance and sometimes with blindness.

Coloboma

Coloboma is a rare congenital orbital anomaly characterized by herniation of the retina through a choroidal defect, creating a cystic pouch within the eye. Another definition for coloboma is absence of some ocular tissue, usually due to malclosure of the fetal intraocular fissure.

The disease has an autosomal dominant mode of inheritance.

Three types of colobomas are found:

- **Optic disc coloboma (morning glory syndrome):**

The defect occurs at the optic disc. On fundoscopy, there is enlargement and excavation of the optic disc, which has pale glial tissue in its floor, and is surrounded by an annulus of pigmented choroidal tissue. This appearance is typical for optic disc coloboma (Fig. 2.11.1). The rest of the eye can be normal or microphthalmic.

The disease is diagnosed in the first year of life due to strabismus (the eyes are not properly aligned with each others) and poor vision.



Fig. 2.11.1 Illustration shows the typical fundoscopic appearance of the optic disc coloboma “morning glory syndrome”

Optic nerve coloboma is usually associated with other anomalies such as optic nerve atrophy, fronto-phenoidal encephalocele, and craniosynostosis.

Differential diagnosis of optic nerve coloboma

- **Staphyloma:** a localized, inflammatory expansion (ectasia) of the globe. It lacks the fundoscopic characteristic feature of the optic nerve coloboma.
- **Microphthalmos with cyst:** is a condition characterized by severe malformation of the globe with gross scleral dilatation forming a cyst that can exceed the size of the globe. An important feature on CT is that the cyst neck is smaller than the cyst itself (not as wide as the coloboma).

Signs on Orbital CT

- There is cystic expansion of the optic nerve, which is isodense and is continuous with the vitreous humor (Fig. 2.11.2).
- Calcification of the optic nerve can be seen in cases of nerve atrophy.
- Microphthalmia may or may not be found.

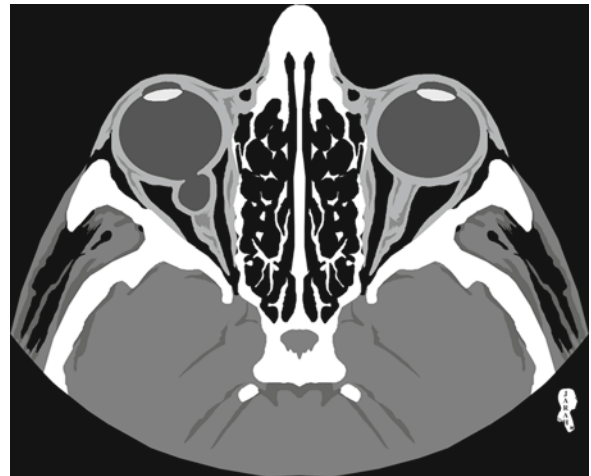


Fig. 2.11.2. Axial orbital CT illustration shows cystic expansion of the right optic disc (optic disc coloboma)

- **Megarbane syndrome:** is a syndrome characterized by microcephaly, coloboma of the iris and optic disc, strabismus, and mental retardation.
- **Retinochoroidal coloboma:** Retinochoroidal coloboma occurs in the inferior aspect of the eye near the optic disc. It is bilateral in up to 60% of cases.

Signs on Orbital CT

The scan shows a small globe (microphthalmia) with a retroocular cyst that is connected to the vitreous humor inferiorly.

Fuch's coloboma (tilted disc syndrome) Fuch's coloboma is a rare congenital malformation characterized by tilting of the optic disc in any direction, with myopia, and minor dilatation of the inferionasal area of the globe due to scleral thinning.

The disease is bilateral in 80% of patients.

There is an association between Fuch's coloboma and craniopharyngioma and craniosynostosis.

Signs on Orbital CT

- Moderate to severe hypoplasia of the choroids, retina, and sclera.
- Focal dilatation of the inferionasal posterior wall of the globe, with oblique insertion of the optic nerve and the retinal arteries (Fig. 2.11.3).

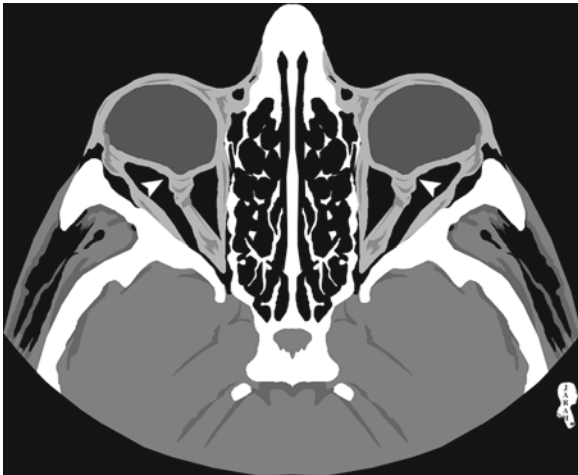


Fig. 2.11.3. Axial orbital CT illustration shows bilateral, abnormal, tilted insertion of the optic nerves into the orbit, a typical sign of “tilted disc syndrome” (*arrowheads*)

Staphyloma

Staphyloma is a condition characterized by bulging of the uvea into a thinned and stretched sclera. It commonly

occurs in the posterior aspect of the globe at the temporal side of the optic disc.

Staphyloma is commonly associated with congenital myopia, a condition characterized by painless bulging eye and amblyopia (poor vision in a physically normal eye).

Signs on Orbital CT

The scan shows a focal posterior or anterior bulge within the eye, and an area of thinning or absence of the scleral–uveal rim (Fig. 2.11.4). There is no contrast enhancement after contrast material injection.

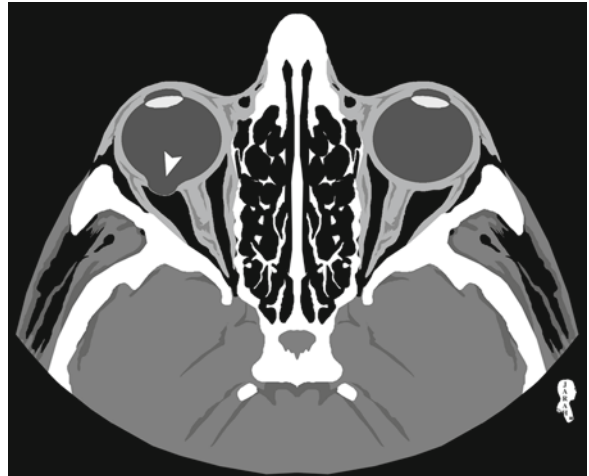


Fig. 2.11.4. Axial orbital CT illustration shows thinning of the scleral–uveal region of the right globe, representing a classic sign of staphyloma (*arrowhead*)

Coats Disease

Coats disease is a rare congenital, idiopathic, nonfamilial disease characterized by an abnormal blood–retinal barrier of the retinal arteries, resulting in leakage of yellowish exudates rich in cholesterol crystals into the vessel wall. Weakening of the blood vessel wall causes the formation of telangiectases (chronic dilatation of groups of capillaries), aneurysms, and subretinal leakage (Fig. 2.11.5), all of which lead to retinal detachment.

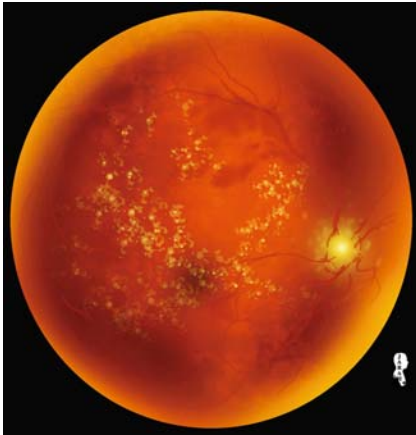


Fig. 2.11.5. Illustration shows the typical fundoscopic appearance of Coats disease. Note the intravitreal hemorrhage and yellowish exudates, which result in a hyperdense and hyperintense appearance of the globe on both CT and MR images

The mean age of presentation is between 3 and 9 years of age.

The disease is unilateral in 80% of cases, and affects men in 70% of cases.

The main signs of the disease are strabismus and leukokoria (white pupillary reflex when one shines a bright light on the pupil; it normally appears red).

The main indication for orbital CT is to differentiate retinoblastoma from chronic Coats disease by searching for intraocular calcifications (very commonly seen in retinoblastoma).

Signs on CT and MRI

- The vitreous humor in the affected eye is homogeneously hyperdense on CT, and hyperintense on T1-weighted and T2-weighted MR images due to exudates and hemorrhage (Fig. 2.11.6).
- Absence of intraocular mass (retinoblastoma presents as intraocular mass).
- Absence of intraocular calcification (calcification in retinoblastoma is very common).
- Partial or incomplete retinal detachment in advanced stages.

Optic Disc Drusen

Optic disc drusen is a rare disease characterized by deposition of hyaline-like material on or near the surface of the optic disc, subsequently resulting in optic disc calcification. It occurs in about 1% of the population.

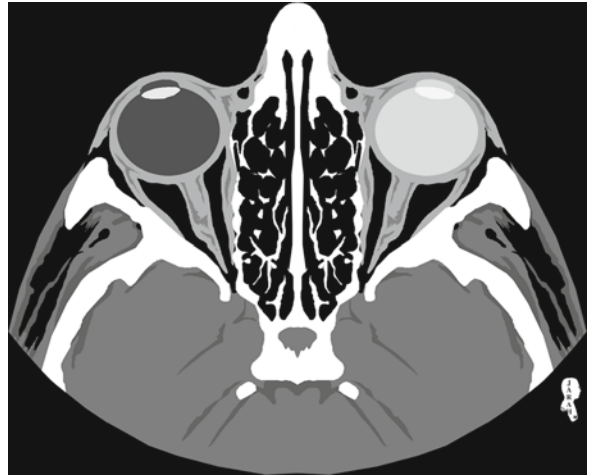


Fig. 2.11.6. Axial orbital CT illustration shows homogeneously hyperdense left globe with absence of a mass lesion, a typical finding in Coats disease

The mean age of presentation is about 12 years of age (hyaline proteins take time to deposit and calcify). The disease is familial, and sometimes discovered accidentally on ophthalmoscopic or CT examinations. Up to 70% of cases are bilateral. Patients present with visual field defects in 80% of cases and with migraine-like headache in up to 30% of cases.

Signs on CT

The scan shows bilateral calcification of the optic disc (Fig. 2.11.7).



Fig. 2.11.7. Axial orbital CT illustration shows bilateral calcification of the optic nerves in optic disc Drusen disease (arrowheads)

Persistent Hyperplastic Primary Vitreous

In the embryo, the primary vitreous occupies the space between the lens and the retina, and it is supplied by a branch from the posterior ophthalmic artery called “the hyaloid artery” in the third week of gestation. Later in life, the primary vitreous is replaced by a secondary vitreous and the hyaloid artery regresses by the third trimester. Persistent hyperplastic primary vitreous (PHPV) represents a condition characterized by persistent proliferation of the primary vitreous due to persistence of the hyaloid artery supplying it (Fig. 2.11.8).

PHPV is a disease of infants, and occurs in a unilateral eye. The infant presents with microphthalmia and leukokoria (white papillary reflex). PHPV is the second most common cause of leukokoria after retinoblastoma.

Signs on Orbital CT

- The affected eye is microphthalmic (Fig. 2.11.9).
- Generalized increase in the vitreous density in the affected eye (Fig. 2.11.9).
- An irregular mass with posterior vitreous extensions present at the area of the lens (Fig. 2.11.9).
- The lens is deformed and misshaped, with no signs of calcification. The lens may be replaced by fat (Fig. 2.11.8).
- Retinal detachment may be present.
- Enhancement of the abnormal vitreous mass after contrast material administration.
- Triangular, cylindrical, or tubular intraventricular densities representing remnant of the primary vitreous (Fig. 2.11.9).

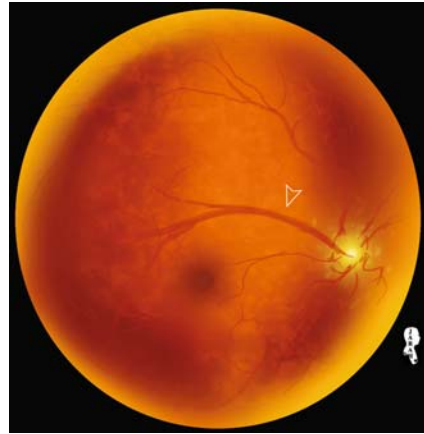


Fig.2.11.8. Illustration shows the fundoscopic appearance of the persistent hyaloids artery in PHPV (*open arrowhead*)

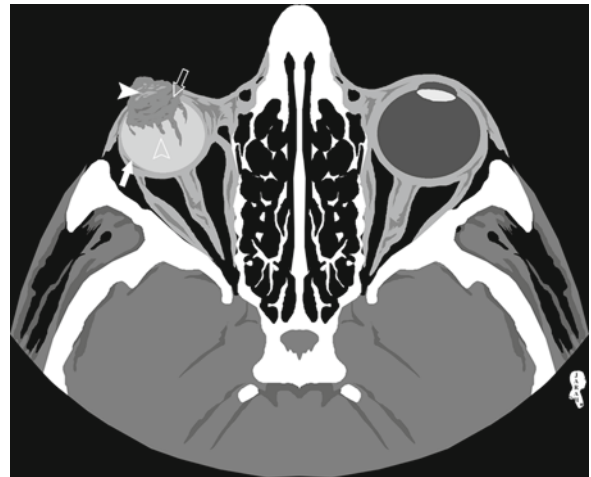


Fig.2.11.9. Axial orbital CT illustration shows the typical findings in PHPV. Note the small size of the eye (*white arrow*), the irregular mass with posterior vitreous extensions present at the area of the lens (*open arrow*), the deformed lens (*white arrowhead*), and the tubular intraventricular densities representing remnants of the primary vitreous (*open arrowhead*). Also, note the hyperdense vitreous humor of the affected right globe compared to the normal left globe

Retinopathy of Prematurity (Retrolental Fibroplasias)

Retinopathy of prematurity is a disease that occurs in premature babies due to abnormal growth of blood vessels within the retina, and fibroblastic overgrowth of a persistent vascular sheath behind the lens as a consequence of premature birth. The disease can progress rapidly within a few weeks resulting in complete blindness.

The disease has similar manifestations and radiological findings to PHPV, but characteristically affects both eyes bilaterally and symmetrically (whereas PHPV affects a single globe). When PHPV occurs in both globes, the only criterion with which to differentiate it from retinopathy of prematurity is the history of the patient.

The disease has a correlation with high oxygen therapy due to prematurity.

Diagnostic criteria:

- History of prematurity with admission to intensive care unit and oxygen therapy.
- Bilateral disease with small globe (Fig. 2.11.10).

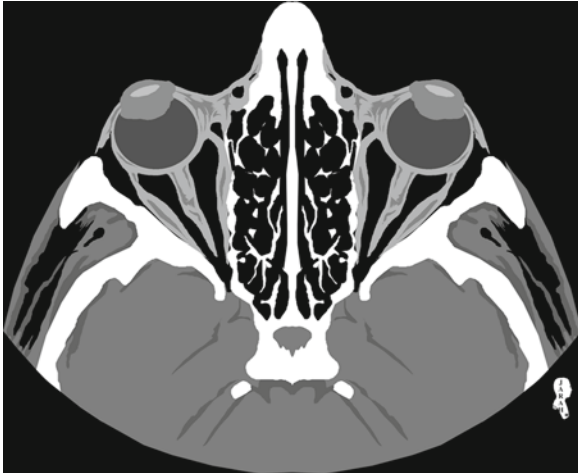


Fig. 2.11.10. Axial orbital CT illustration shows bilateral microphthalmia with masses seen around the lens in the same pattern as PHPV. These findings plus history of prematurity and oxygen therapy are diagnostic criteria for retinopathy of prematurity

For Further Reading

1. Mafee MF et al. Computed tomography of optic nerve colobomas, morning glory anomaly, and colobomatous cyst. *Radiol Clin North Am* 1987;25(4):693–699
2. Manfre L et al. Bitemporal pseudohemianopia related to the “tilted disk” syndrome: CT, MR, and fundoscopic findings. *Am J Neuroradiol* 1999;20:1750–1751
3. Chen CS et al. Morning glory syndrome and basal encephalocele. *Child Nerv Syst* 2004;20:87–90
4. Doglietto F et al. Microphthalmia and colobomatous cyst of the orbit. *Acta Neurochir (Wien)* 2006;148:1123–1125
5. Murphy BL et al. Optic nerve coloboma (morning glory syndrome): CT findings. *Radiology* 1994;191:59–61
6. Belden CJ. MR imaging of the globe and optic nerve. *Neuroimag Clin N Am* 2004;14:809–825
7. Galluzzi P et al. Coats disease: Smaller volume of the affected globe. *Radiology* 2001;221:64–69
8. Ramirez H et al. Computed tomographic identification of calcified optic nerve drusen. *Radiology* 1983;148:137
9. Mafee MF et al. Persistent hyperplastic primary vitreous (PHPV): Role of computed tomography and magnetic resonance. *Radiol Clin North Am* 1987;25(4):683–692
10. Okay CA et al. Megarbane syndrome. *Indian J Hum Genet* 2008;14(1):27–29

2.12

Congenital Cholesteatoma

Cholesteatoma is a mass of abnormal squamous epithelium (ectopic skin) found inside the middle ear cavity. When cholesteatoma occurs inside the brain, it is referred to as “epidermoid cyst.”

Up to 98% of cholesteatomas are acquired, only 2% are congenital.

Acquired cholesteatoma arises as a complication of recurrent, chronic otitis media. It originates commonly from the sinus tympani, or Prussak's space, which is the lateral space between the scutum and the ossicles. Cholesteatoma commonly erodes the scutum first, affecting the integrity of the tympanic membrane. It can also erode the tegmen tympani (roof of the middle

ear cavity) causing intracranial extension of the lesion. Patients with acquired cholesteatoma usually present with conductive hearing loss and ear discharge. In contrast, patients with congenital cholesteatoma present with conductive hearing loss and a whitish mass behind an intact tympanic membrane (seen with an otoscope).

Congenital cholesteatoma has the same pathological and radiological features as acquired cholesteatoma, except that it usually occurs in young patients with no history of ear infections.

Congenital cholesteatoma can arise anywhere within the petrous bone, but it is commonly found at the cerebellopontine angle, the petrous apex, the geniculate ganglion region, and the tympanic mastoid cavity.

Congenital cholesteatoma can be mistaken with “cholesterol granuloma” when it affects the petrous apex; differentiation between both lesions can be achieved by MRI.

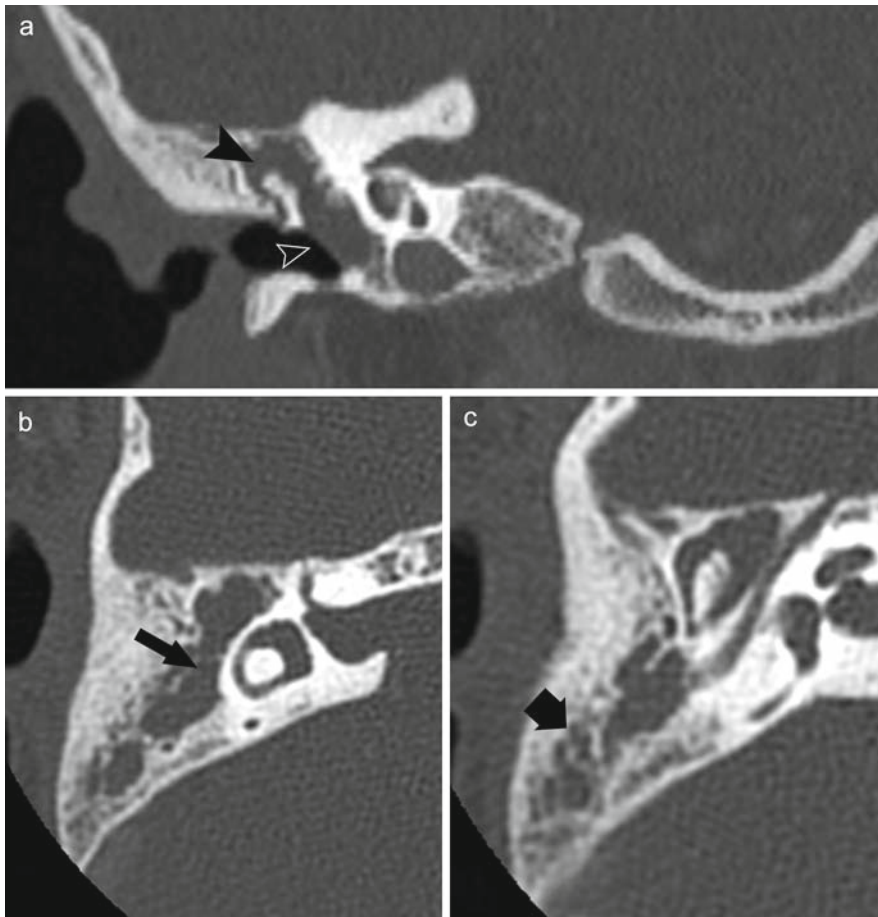


Fig.2.12.1. Coronal and axial postcontrast petrous CT sections in a 9-year-old patient with congenital cholesteatoma. In **a**, there is an isodense opacity filling the middle ear cavity (black arrowhead), with an intact tympanic membrane (open arrowhead). In **b**, the cholesteatoma is seen filling the aditus ad antrum and the mastoid antrum (black arrow). In **c**, the middle ear cavity and the mastoid air cells are fully filled by the cholesteatoma (thick black arrow). Notice lack of enhancement and bone erosions in all sections

Signs on Petrous Bone CT and MR

- An isodense, nondependent soft-tissue opacity seen within the middle ear cavity with opacified mastoid air cells (Fig. 2.12.1).
- The lesions do not enhance after contrast material administration (diagnostic).
- Signs of bone destruction may be seen (e.g., scutum erosions) (Figs. 2.12.2 and 2.12.3).
- Cholesterol granuloma is an inflammatory mass with fatty and hemorrhagic material commonly found at the petrous apex. Cholesteatoma gives low T1 and high T2 signal intensities, while cholesterol granuloma gives high signal intensity in all sequences due to its mix of hemorrhagic–fatty content.



Fig. 2.12.2. Coronal postcontrast petrous CT section in a patient with acquired cholesteatoma. Notice the bony erosion of the tegmen tympani with extension of the cholesteatoma into the middle intracranial fossa (white arrowhead). Notice the lack of enhancement and severe destruction of the ossicles. The cholesteatoma also invades the cochlea forming “labyrinthine fistula” (black arrow)



Fig. 2.12.3. Coronal postcontrast petrous CT section in another patient with acquired cholesteatoma. Notice the large cholesteatoma filling the middle ear cavity, eroding the tegmen tympani (white arrowhead), violating the integrity of the tympanic membrane (open arrowhead), and completely destroying the ossicles (vanished within the mass)

For Further Reading

1. Gok A et al. Congenital cholesteatoma with spontaneous epidural abscess, sinus thrombosis and cavernous fistula. *Neurosurg Rev* 1996;19:189–191
2. Davidson CH. Imaging of the temporal bone. *Neuroimag Clin N Am* 2004;14:721–727

Congenital Diseases and Syndromes

An Illustrated Radiological Guide

Al-Tubaikh, J.A.; Reiser, M.F.

2009, XVII, 201 p.,

ISBN: 978-3-642-00160-4